Characterizing Cortical Folding Patterns Across Species using Prolate Spheroidal Harmonics

D. A. Smith, M. K. Hurdal
dsmith@math.fsu.edu
Department of Mathematics, Florida State University, Tallahassee, Florida 32306-4510

Introduction

Folding patterns of the cerebral cortex have fascinated many generations of scientists. In the past ten years, with the discovery of intermediate progenitor (IP) cells, new hypotheses about how these patterns develop have been introduced. Here, we adopt the intermediate progenitor cell hypothesis [1] (IPH) and developed a new model of the production of IP cells using a Turing reaction-diffusion system. The domain for this model is a prolate spheroid based on the shape of the lateral ventricle.

Here, we start with the development of the cortex and an example of Turing patterns on a one dimensional domain. We then expand the theory to be able to predict evolving patterns on a prolate spheroidal surface. Next, we examine the role that focal distance plays in pattern formation and use it to predict the evolutionary development of cortical patterns in different species.

1. Cortical Development

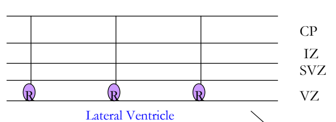

A founding population of radial glial cells (R) is created in the ventricular zone (VZ) located in the lateral wall of lateral ventricle [2].

Radial glial cells (R) go through cycles of asymmetric cellular divisions creating neurons (N) that travel to the cortex creating the lower layers of the cortical plate (CP).

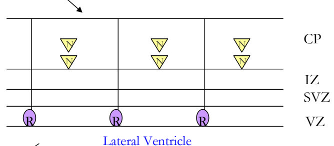

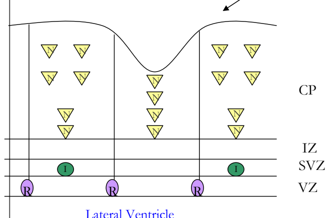

Select radial glial cells (R) switch to cycles of asymmetric cellular divisions creating IP cells (I) that travel to the subventricular zone (SVZ) and create two neurons (N) per cellular division that travel to the cortex. When a subset of "non-activated" radial glial cells is surrounded by subsets of "activated" radial glial cells a sulcus is formed [1].

Since the patterning of IP cells is takes place in the VZ, we are approximating the lateral ventricle with a prolate spheroid and the VZ with a prolate spheroidal surface.

2. Turing patterns on a one-dimensional domain

BVM Model [3] (Barrio, Varea, and Maini)

$$u_t = D\delta\nabla^2 u + \alpha u\left(1 - r_1 v^2\right) + v\left(1 - r_2 u\right)$$

$$v_t = \delta\nabla^2 v + \beta v\left(1 + \frac{\alpha r_1}{\beta} uv\right) + u\left(\gamma + r_2 v\right)$$

Solutions to u are of the form $u = T(t)X(\mathbf{x})$ where $T(t) = e^{\lambda(k^2)t}$ and $X(x)$ is a solution of $\nabla^2 X + k^2 X = 0$ [5].

In one dimension, where $0 < x < \mathrm{P}$, with a periodic boundary condition the solution to $\nabla^2 X + k^2 X = 0$ is $X_k = A_k \cos kx$ and $k^2 = \left(\frac{n\pi}{P}\right)^2$ where n is an integer.

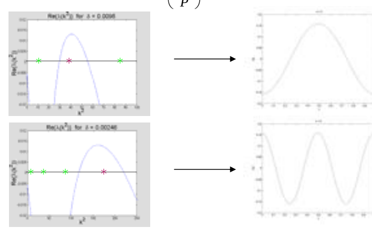

Diffusion driven instability will be accomplished when $\mathrm{Re}(\lambda(k^2)) > 0$. Notice, in the top graph only one k^2 value (corresponding to $n = 2$) will do this. In the second graph, the domain scaling is increased resulting in a shift of the $\mathrm{Re}(\lambda(k^2))$ parabola. Now a larger k^2 value (corresponding to $n = 4$) will be responsible for the pattern.

$d = 0.516$, $r_1 = 3.5$, $r_2 = 0$, $\alpha = 0.899$, $\beta = -0.91$, $\gamma = -0.899$, $\mathrm{P} = 1$

3. Turing Patterns on Prolate Spheroidal Surfaces

Since $X(x)$ is separable in prolate spheroidal coordinates (ξ, η, φ) [6], we can rewrite X in terms of $X_{mn} = R_{mn}(c,\xi) S_{mn}(c,\eta) \Phi_{mn}(\varphi)$ where $c = \frac{1}{2}kd$, d = focal distance, (m,n) are the spheroidal indices, and R and S satisfy

$$\frac{d}{d\eta}\left[\left(1-\eta^2\right)\frac{d}{d\eta}S_{mn}(c,\eta)\right] + \left[\lambda_{mn} - c^2\eta^2 - \frac{m^2}{1-\eta^2}\right]S_{mn}(c,\eta) = 0$$

$$\frac{d}{d\xi}\left[\left(\xi^2-1\right)\frac{d}{d\xi}R_{mn}(c,\xi)\right] - \left[\lambda_{mn} - c^2\xi^2 + \frac{m^2}{\xi^2-1}\right]R_{mn}(c,\xi) = 0$$

Since the domain is a prolate spheroidal surface, the solution is radially invariant, i.e. $\frac{dR}{d\xi} = 0$, and we obtain an equation (1) that relates k^2 with the (m,n) pattern obtained.

$$k^2 = \underbrace{\frac{4}{d^2}\left(\lambda_{mn}\left(\frac{1}{2}kd\right) + \frac{m^2}{\xi_0^2 - 1}\right)}_{A_{mn}} \qquad (1)$$

where ξ_0 conserves a surface area of 4π.

4. Simulations on a Prolate Spheroidal Surface

With a fixed focal distance, A_{mn} (the right hand side of (1)) can be plotted versus k for each (m,n). Below are two simulations on a prolate spheroid with focal distance of one and parameters given below. The top simulation has a domain scaling corresponding to $k^2 = 30$. Notice, $k^2 = 30$ (lower star) corresponds to A_{35} and verifies the pattern obtained. The bottom simulation corresponds to $k^2 = 60$ (top star) and verifies the pattern predicted of A_{77}.

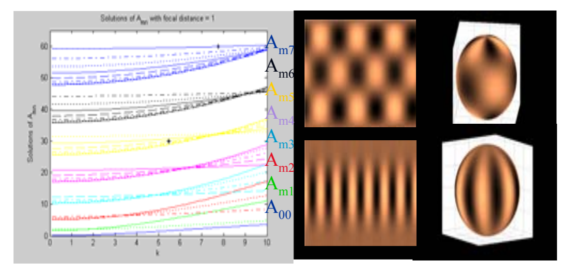

Computer modeling verification of spheroidal mode equation (Equation (1)). A.) Graph of A_{mn} for $n = 0, .., 7$ (different colors) and $m = 0, .., n$ (different linestyles, beginning with $m = 0$ on the bottom and $m = n$ on top) . When $k^2=30$ and 60 the corresponding patterns are A_{35} and A_{77}, respectively. **B**.) Results of discretization of BVM system for $\delta = 0.013$ (corresponding to $k^2=30$), $\alpha = 0.899$, $\beta = -0.91$, $\gamma = -0.899$, $D = 0.5319$, $r_1 = 3.5$, and $r_2 = 0$. **C**.) Projection of B onto a prolate spheroid ($d = 1$) such that top (bottom) edge maps to the north (south) pole of the spheroid. **D**. & **E**.) Same as **B & C** except $\delta = 0.0065$ (corresponding to $k^2 = 60$).

5. Evolutionary Development

Evolutionarily the cerebral cortex and lateral ventricle have expanded greatly. The expansion of the lateral ventricle is captured with the focal distance (d) of the prolate spheroid. Here we are plotting the curves A_{11}, A_{02}, and A_{04}. The pattern A_{11} corresponds to the pattern needed to create one sulcus sectorially (following along the major axis of the lateral ventricle). A_{02} corresponds to one sulcus forming a ring around the lateral ventricle and A_{04} corresponds to 2 sulcal rings.

Notice in Graph A as k^2 increases the first pattern it will intersect is A_{11}. If d is increased (B), the curves shift and now as k^2 increases it will intersect A_{02} before A_{11}, therefore a one sulcal ring could form before a sectorial sulcus. If d is increased further (C), as k^2 increases it will intersect A_{04} before A_{11} meaning 2 ring sulci could form before the first sectorial sulcus. These scenarios are similar to what occurs in the cat, lemur, and human.

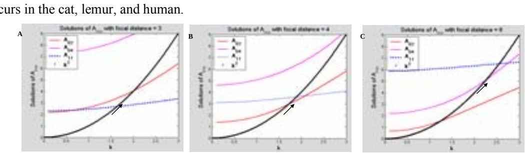

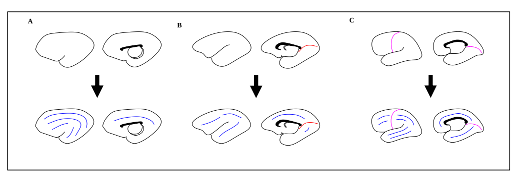

Predicted development of folds in cortices of 3 species. In the bottom figure, the top row shows the formation of sulcal rings. The bottom row shows the subsequent creation of a certain number of sectorial sulci for **A**. cat (modified from [7]) **B**. Lemur (modified from [8]) **C**. Human (modified from [8]).

Literature cited

1. A. Kriegstein, S. Noctor, V. Martinez-Cerdeno, *Nature Reviews Neuroscience*, **7(11)**, 883-890 (2006).
2. P. Rakic, *Science* **241**, 170-176, (1988).
3. R.A. Barrio, C. Varea, J. L. Aragon, P. K. Maini, *Bulletin of Mathematical Biology*, **61(3)**, 483-505 (1999).
4. A.M. Turing, *Philosophical Transactions of the Royal Society of London B*, **237**, 37-72 (1952).
5. J. D. Murray, *Mathematical Biology* (Springer, New York, ed. 2, 1989).
6. C. Flammer, *Spheroidal Wave Functions* (Stanford Univ. Press, Palo Alto, 1957).
7. J Reighard, H. S. Jennings, *Anatomy of the Cat* (Holt, Rinehart and Winston, ed. 3, 1935).
8. K. Brodmann, *Brodmann's Localisation in the cerebral cortex* (Springer, New York, 2006).

Acknowledgments and Further Information

We would like to thank the Association for Women in Mathematics for travel funding to present this work. We would also like to thank Richard Bertram, Juan B. Gutierrez, David Kopriva, Washington Mio, Jack Quine, Andre Striegel, and DeWitt Sumners for their valuable comments and support.

For further information please contact *dsmith@math.fsu.edu*
For information on related projects please see:
www.math.fsu.edu/~mhurdal